Fulde-Ferrell superfluidity in ultracold Fermi gases with Rashba spin-orbit coupling

Hui Hu[1] and Xia-Ji Liu[1*]
[1]*Centre for Atom Optics and Ultrafast Spectroscopy,*
Swinburne University of Technology, Melbourne 3122, Australia
(Dated: September 3, 2018)

We theoretically investigate the inhomogeneous Fulde-Ferrell (FF) superfluidity in a three dimensional atomic Fermi gas with Rashba spin-orbit coupling near a broad Feshbach resonance. We show that within mean-field theory the FF superfluid state is always more favorable than the standard Bardeen-Cooper-Schrieffer (BCS) superfluid state when an in-plane Zeeman field is applied. We present a qualitative finite-temperature phase diagram near resonance and argue that the predicted FF superfluid is observable with experimentally attainable temperatures (i.e., $T \sim 0.2T_F$, where T_F is the characteristic Fermi degenerate temperature).

I. INTRODUCTION

The Fulde-Ferrell (FF) superfluid is a fascinating state proposed to understand the fermionic superfluidity with unequal populations in the two spin states [1]. Unlike the standard Bardeen-Cooper-Schrieffer (BCS) superfluid, where fermions of opposite spin and momentum form Cooper pairs and condense into a microscopic state at rest, the FF superfluid is characterized by Cooper pairs carrying a single-valued center-of-mass momentum and thus by an inhomogeneous condensate state. More complicated inhomogeneous condensate states are also possible with the inclusion of more center-of-mass momenta for their spatial structure in real space, as suggested by Larkin and Ovchinnikov (LO) [2]. These forms of inhomogeneous superfluidity have now been collectively referred to as FFLO superfluids. They are anticipated to have manifestations in a number of important physical settings, ranging from solid-state superconductors to the nuclear matter at the heart of neutron stars [3–5]. However, despite tremendous theoretical and experimental efforts over the past fifty years, conclusive experimental evidence of their existence remains elusive [3–17]. In this work, we show that the long-sought FF superfluid might be observable in a three dimensional (3D) ultracold atomic Fermi gas with Rashba spin-orbit coupling and in-plane Zeeman field.

The idea that inhomogeneous superfluidity is enhanced by Rashba spin-orbit coupling was first suggested by Barzykin and Gor'kov in the study of surface superfluidity in materials such as WO$_3$:Na [18, 19] and was later generalized to a 3D Fermi system by Agterberg and Kaur [20]. It was recently revisited by Zheng and co-workers in the context of ultracold atomic Fermi gases [21, 22], which have the unique experimental advantage of unprecedented controllability in interactions, spin-populations and purity [23]. In contrast to solid-state superconductors, ultracold atomic Fermi gases are gen-
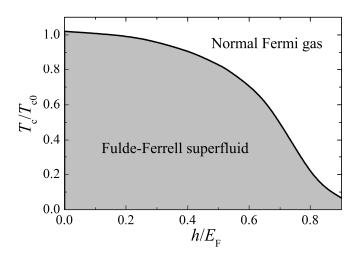

Figure 1: (color online) Finite temperature phase diagram of a 3D Rashba spin-orbit coupled atomic Fermi gas at a broad Feshbach resonance ($1/k_F a_s = 0$) and at the spin-orbit coupling strength $\lambda k_F/E_F = 1$. Here, $k_F = (3\pi^2 n_F)^{1/3}$ and $E_F = \hbar^2 k_F^2/(2m)$ are the Fermi wavevector and Fermi energy, respectively, expressed in terms of the gas density n_F. The critical temperature, in units of the mean-field critical temperature without spin-orbit coupling $T_{c0} \simeq 0.496T_F = 0.496E_F/k_B$, decreases monotonically with increasing the in-plane Zeeman field h.

erally prepared in the strongly interacting regime [5], the so-called crossover regime from a Bose-Einstein condensate (BEC) to a BCS superfluid, in order to have an experimentally attainable superfluid transition temperature. As a result, the theoretical investigation of inhomogeneous superfluidity in such ultracold matter has to rely on heavy numerical calculations within mean-field theory. In the previous work by Zheng and co-workers [21], the FF superfluidity has been addressed at zero temperature along the BEC-BCS crossover. Here, we present a qualitative mean-field phase diagram at finite temperatures and show that the FF superfluid state might be within reach at the typical experimental temperature $T \sim 0.2T_F \simeq 0.4T_{c0}$, where T_F is the Fermi degenerate temperature and $T_{c0} \simeq 0.496T_F$ is the mean-field
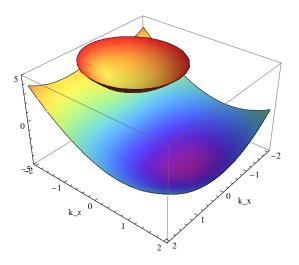
Figure 2: (color online) Schematic of the Fermi surfaces of a Rashba spin-orbit coupled with in-plane Zeeman field along the z-axis.

critical temperature of a resonantly interacting (unitary) Fermi gas without spin-orbit coupling. We note that the mean-field theory gives only a qualitative estimate of the superfluid transition temperature. For example, for a unitary gas, the mean-field prediction of $T_{c0} \simeq 0.496 T_F$ is significantly larger than an experimental measurement $T_{c0} \simeq 0.167(13) T_F$ [24].

Our main result is summarized in Fig. 1, where the phase transition temperature to a normal state is shown as a function of the in-plane Zeeman field, for a strongly interacting Rashba spin-orbit coupled Fermi gas at a broad Feshbach resonance. We find that the FF superfluid is always the true ground state at a finite Zeeman field.

The significantly enlarged parameter space for a FF superfluid can be qualitatively understood from the change of the two Fermi surfaces due to spin-orbit coupling, as discussed by Barzykin and Gor'kov [18] and by Agterberg and Kaur [20]. Here we explain very briefly the physical picture following their ideas. We consider the spin-oribt coupling $\lambda(\sigma_x \hat{k}_x + \sigma_z \hat{k}_z)$ together with an in-plane Zeeman field along the z-direction $h\sigma_z$, for which the single-particle energy spectrum takes the form,

$$E_{\mathbf{k}\pm} = \frac{\hbar^2 k^2}{2m} \pm \sqrt{\lambda^2 k_x^2 + (\lambda k_z + h)^2}, \qquad (1)$$

where "$\pm$" accounts for two helicity branches. The atom in each branch stays at a *mixed* spin state.

At relatively large spin-orbit coupling (i.e., $\lambda k_F \gg h$), we may approximate

$$E_{\mathbf{k}\pm} \simeq \frac{\hbar^2 \left(k_x^2 + k_y^2\right)}{2m} + \frac{\hbar^2}{2m}\left(k_z \pm \frac{q}{2}\right)^2 \pm \lambda\sqrt{k_x^2 + k_z^2}, \quad (2)$$

where

$$q = \frac{2mh}{\hbar^2 \sqrt{k_x^2 + k_z^2}}. \qquad (3)$$

It is easy to see that the centers of the two Fermi surfaces in different branch are shifted by $(q/2)\mathbf{e}_z$ along the z-axis in opposite directions, as shown in Fig. 2, where $\mathbf{e}_z$ is the unit vector along the z-axis. Thus, if the fermionic pairing occurs in the lower helicity branch, it would pair two atoms staying at the single-particle states of $\mathbf{k} + (q/2)\mathbf{e}_z$ and $-\mathbf{k} + (q/2)\mathbf{e}_z$, respectively, giving rise to a FF order parameter that has a spatial dependence $\Delta(\mathbf{x}) = \Delta e^{iqz}$ [20]. This pairing mechanism holds for arbitrary small in-plane Zeeman field and explains why the FF superfluid is always more preferable than the standard BCS superfluid at large spin-orbit coupling. The direction of the FF momentum is uniquely determined by the form of spin-orbit coupling and its magnitude is roughly proportional to the in-plane Zeeman field h if h is small, i.e., see Eq. (3).

Let us now consider small spin-orbit coupling. In the absence of spin-orbit coupling, the formation of an inhomogeneous superfluid is driven by the population imbalance, which also leads to the distortion of the Fermi surfaces. In that case, there are many equivalent ways to deform the surfaces. As a result, the direction of the single FF pairing momentum is not specified. Thus, for any FF superfluid solution with a pairing momentum $+\mathbf{q}$, we can always find another degenerate solution with the pairing momentum $-\mathbf{q}$. This indicates that a stripe LO phase with an order parameter in the form of $\cos(\mathbf{q} \cdot \mathbf{x})$ will be more favorable, which is simply a superposition of the $+\mathbf{q}$ and $-\mathbf{q}$ plane waves. The investigation of the LO phase in a 3D Fermi gas without spin-orbit coupling has been carried out by Burkhardt and Rainer many years ago [25] and recently by a number of authors [26, 27]. In the presence of spin-orbit coupling, the two solutions with the $+\mathbf{q}$ and $-\mathbf{q}$ plane waves are no longer degenerate. Numerically, we find that one solution becomes more favorable and the energy difference between the two solutions increases rapidly with increasing spin-orbit coupling. Therefore, with increasing spin-orbit coupling, we anticipate the LO phase will cease to exist and the large spin-orbit coupling will uniquely determine a single-valued pairing momentum and lead to a FF superfluid. The competition between LO and FF phases in a Rashba spin-orbit coupled 3D Fermi gas was recently investigated by Agterberg and Kaur [20]. The stripe LO phase was found to cease to exist at large population imbalance.

It is important to note that the experimentally realized spin-orbit coupling is not of the pure Rashba type [28, 29]. Instead, it is an equal weight combination of the Rashba and Dresselhaus spin-orbit couplings (for a detailed discussion, see for example, Ref. [30]). The possibility of observing FF superfluidity in current experimental settings has been discussed by Shenoy [31], the present authors [32], and also by Wu and co-workers but in two dimensions [33]. We anticipate that the Rashba spin-orbit coupling might be experimentally realized soon [36, 37]. Furthermore, it is also feasible to create a 3D isotropic spin-orbit coupling [37, 38]. The FF superfluidity with 3D isotropic spin-orbit coupling has been inves-

tigated most recently by Dong and co-workers [34] and by Zhou and colleagues [35].

The reminder of the paper is organized as follows. In Sec. II we introduce the model Hamiltonian for a Rashba spin-orbit coupled Fermi gas with an in-plane Zeeman field and describe the mean-field framework. We present the explicit expression of the mean-field thermodynamic potential, with the FF pairing momentum q and pairing order parameter Δ as the variational parameters. In Sec. III, we discuss in detail competing ground states near a broad Feshbach resonance and show that the FF superfluid is always the true ground state at finite Zeeman fields in the superfluid phase. We explore systematically the properties of this exotic state of matter at finite temperatures. In Sec. IV we present our conclusions. For the convenience of numerical calculations, we use a non-standard form of Rashba spin-orbit coupling. In the Appendix A, we show that it is fully equivalent to the Rashba spin-orbit coupling commonly used in the literature.

II. MODEL HAMILTONIAN

We consider a 3D spin-1/2 Fermi gas of ^{6}Li or ^{40}K atoms near broad Feshbach resonances with Rashba-type spin-orbit coupling $\lambda(\sigma_x \hat{k}_x + \sigma_z \hat{k}_z)$ and an in-plane Zeeman field along the z-direction $h\sigma_z$, a configuration to be experimentally realized in the future [36, 37]. Here σ_x and σ_z are the Pauli matrices, $\hat{k}_x \equiv -i\partial_x$ and $\hat{k}_z \equiv -i\partial_z$ are the momentum operators. In the Appendix A, we discuss in more detail about the expression of Rashba spin-orbit coupling. The model Hamiltonian of the system may be described by

$$\mathcal{H} = \int d\mathbf{x} \left[\mathcal{H}_0(\mathbf{x}) + \mathcal{H}_{\text{int}}(\mathbf{x}) \right], \tag{4}$$

where the single-particle Hamiltonian takes the form

$$\mathcal{H}_0 = \left[\psi_\uparrow^\dagger, \psi_\downarrow^\dagger \right] \begin{bmatrix} \hat{\xi}_\mathbf{k} + \lambda \hat{k}_z + h & \lambda \hat{k}_x \\ \lambda \hat{k}_x & \hat{\xi}_\mathbf{k} - \lambda \hat{k}_z - h \end{bmatrix} \begin{bmatrix} \psi_\uparrow \\ \psi_\downarrow \end{bmatrix} \tag{5}$$

and the pairing interaction Hamiltonian is given by

$$\mathcal{H}_{\text{int}} = U_0 \psi_\uparrow^\dagger(\mathbf{x}) \psi_\downarrow^\dagger(\mathbf{x}) \psi_\downarrow(\mathbf{x}) \psi_\uparrow(\mathbf{x}), \tag{6}$$

describing the contact interaction between the two spin states with interaction strength U_0. In the above Hamiltonian, $\psi_\sigma^\dagger(\mathbf{x})$ and $\psi_\sigma(\mathbf{x})$ are respectively the creation and annihilation field operators for atoms in the spin-state σ, and $\hat{\xi}_\mathbf{k} \equiv -\hbar^2 \nabla^2/(2m) - \mu$ is the single-particle kinetic energy with atomic mass m in reference to the chemical potential μ. We have denoted the strength of Rashba spin-orbit coupling and of in-plane Zeeman field by λ and h, respectively. The use of the contact interatomic interaction generally leads to an ultraviolet divergence at large momentum and high energy. To remove

such a divergence, it is useful to express the interaction strength U_0 in terms of the s-wave scattering length a_s,

$$\frac{1}{U_0} = \frac{m}{4\pi\hbar^2 a_s} - \frac{1}{V} \sum_\mathbf{k} \frac{m}{\hbar^2 k^2}, \tag{7}$$

where V is the volume of the system. In principle, the scattering length a_s may be tuned precisely to arbitrary value, by sweeping an external magnetic field across the Feshbach resonance [23]. However, in the proposed schemes for creating Rashba spin-orbit coupling [36, 37], the magnetic bias field must be fine-tuned to adjust the energy levels of the hyperfine states. This means that the scattering length for a particular type of atoms may be restricted to the weak-coupling regime, in which we know that without spin-orbit coupling it is difficult to have an experimentally accessible superfluid transition temperature. Nevertheless, the many-body pairing could be significantly enhanced by Rashba spin-orbit coupling [39–44]. By properly tuning the Rashba spin-orbit coupling strength, which in some sense equivalent to tuning the scattering length [44], we do anticipate a sizable superfluid transition temperature.

A. Mean-field Bogoliubov-de Gennes theory

A solid-state Fermi system with Rashba spin-orbit coupling and in-plane Zeeman field provides a promising platform to observe the long-sought FFLO superfluid, as suggested by Barzykin and Gor'kov in their pioneering work [18]. In the context of ultracold atomic Fermi gases, this idea was renewed, as motivated by the interesting finding that the two-body bound state of the model Hamiltonian acquires a finite center-of-mass momentum along the z-axis [45]. This strongly indicates the existence of a FF pairing state with a single-valued center-of-mass momentum at the many-body level [31]. Indeed, in a recent zero-temperature calculation by Zheng and co-workers [21], the parameter space of the FF superfluid has been found to be significantly enhanced by the Rashba spin-orbit coupling. Here we explore the whole mean-field phase diagram at finite temperatures.

Let us assume an order parameter with a single-valued center-of-mass momentum along the z-axis:

$$\Delta(\mathbf{x}) = -U_0 \langle \psi_\downarrow(\mathbf{x}) \psi_\uparrow(\mathbf{x}) \rangle = \Delta e^{iqz}. \tag{8}$$

The direction of the FF pairing momentum is chosen following the center-of-mass momentum of the two-particle ground state [45]. It is also consistent with the previous mean-field studies for Rashba spin-orbit coupled Fermi systems [18, 20, 21]. Within mean-field theory, we approximate the interaction Hamiltonian by,

$$\mathcal{H}_{\text{int}} \simeq - \left[\Delta(\mathbf{x}) \psi_\uparrow^\dagger(\mathbf{x}) \psi_\downarrow^\dagger(\mathbf{x}) + \text{H.c.} \right] - \frac{\Delta^2}{U_0}. \tag{9}$$

For a Fermi superfluid, it is convenient to use the following Nambu spinor representation for the field operators,

$$\Phi(\mathbf{x}) \equiv \left[\psi_\uparrow(\mathbf{x}), \psi_\downarrow(\mathbf{x}), \psi_\uparrow^\dagger(\mathbf{x}), \psi_\downarrow^\dagger(\mathbf{x})\right]^T, \quad (10)$$

where the first two and last two field operators in $\Phi(\mathbf{x})$ could be interpreted as the annihilation operators for particles and holes, respectively. The total Hamiltonian can then be written in a compact form,

$$\mathcal{H} = \frac{1}{2} \int d\mathbf{x}\,\Phi^\dagger(\mathbf{x})\mathcal{H}_{BdG}\Phi(\mathbf{x}) - V\frac{\Delta^2}{U_0} + \sum_{\mathbf{k}} \hat{\xi}_{\mathbf{k}}, \quad (11)$$

where the factor of $1/2$ in the first term arises from the double use of particle and hole operators in the Nambu spinor $\Phi(\mathbf{x})$. Accordingly, a zero-point energy $\sum_{\mathbf{k}} \hat{\xi}_{\mathbf{k}}$ appears in the last term, which is formally divergent. The Bogoliubov Hamiltonian $\mathcal{H}_{BdG}$ takes the form,

$$\mathcal{H}_{BdG} \equiv \begin{bmatrix} \hat{\xi}_{\mathbf{k}} + \lambda\hat{k}_z + h & \lambda\hat{k}_x & 0 & -\Delta(\mathbf{x}) \\ \lambda\hat{k}_x & \hat{\xi}_{\mathbf{k}} - \lambda\hat{k}_z - h & \Delta(\mathbf{x}) & 0 \\ 0 & \Delta^*(\mathbf{x}) & -\hat{\xi}_{\mathbf{k}} + \lambda\hat{k}_z - h & \lambda\hat{k}_x \\ -\Delta^*(\mathbf{x}) & 0 & \lambda\hat{k}_x & -\hat{\xi}_{\mathbf{k}} - \lambda\hat{k}_z + h \end{bmatrix}. \quad (12)$$

In free space, where the momentum is a good quantum number, it is straightforward to diagonalize the Bogoliubov Hamiltonian

$$\mathcal{H}_{BdG}\Phi_{\mathbf{k}\eta}(\mathbf{x}) = E_{\mathbf{k}\eta}\Phi_{\mathbf{k}\eta}(\mathbf{x}), \quad (13)$$

by using the plane-wave quasiparticle wave-function

$$\Phi_{\mathbf{k}\eta}(\mathbf{x}) = \frac{1}{\sqrt{V}}e^{i\mathbf{k}\cdot\mathbf{x}}[u_{\mathbf{k}\eta\uparrow}e^{+iqz/2}, u_{\mathbf{k}\eta\downarrow}e^{+iqz/2}, v_{\mathbf{k}\eta\uparrow}e^{-iqz/2}, v_{\mathbf{k}\eta\downarrow}e^{-iqz/2}]^T \quad (14)$$

and quasiparticle energy $E_{\mathbf{k}\eta}$. The Bogoliubov Hamiltonian now becomes a 4 by 4 matrix and the four eigenvalues and eigenstates have been specified using the index η ($\eta = 1, 2, 3, 4$).

The mean-field thermodynamic potential Ω at a temperature T is then given by

$$\frac{\Omega}{V} = \frac{1}{2V}\left[\sum_{\mathbf{k}}(\xi_{\mathbf{k}+\mathbf{q}/2} + \xi_{\mathbf{k}-\mathbf{q}/2}) - \sum_{\mathbf{k}\eta} E_{\mathbf{k}\eta}\right] - \frac{k_B T}{V}\sum_{\mathbf{k}\eta}\ln\left(1 + e^{-E_{\mathbf{k}\eta}/k_B T}\right) - \frac{\Delta^2}{U_0}, \quad (15)$$

where the zero-point energy $\sum_{\mathbf{k}\eta} E_{\mathbf{k}\eta}$ in the first term (i.e., the square bracket) is again due to the double use of particle and hole operators, and the zero-point energy $\sum_{\mathbf{k}} \hat{\xi}_{\mathbf{k}}$ has been rewritten as $\sum_{\mathbf{k}}(\xi_{\mathbf{k}+\mathbf{q}/2} + \xi_{\mathbf{k}-\mathbf{q}/2})/2$ to cancel the divergence in $\sum_{\mathbf{k}\eta} E_{\mathbf{k}\eta}$. The second term in the above thermodynamic potential accounts for the thermal excitations of Bogoliubov quasiparticles, which do not interact with each other in the mean-field approximation. It should be noted that, the summation over the quasiparticle energy in $\sum_{\mathbf{k}\eta}$ must be restricted to $E_{\mathbf{k}\eta} \geq 0$, because of an inherent particle-hole symmetry in the Nambu spinor representation. For instance, it is straightforward to check that for any particle state $[u_{\mathbf{k}\uparrow}, u_{\mathbf{k}\downarrow}, v_{\mathbf{k}\uparrow}, v_{\mathbf{k}\downarrow}]^T$ with energy $E_{\mathbf{k}} \geq 0$, there is a one-to-one corresponding hole state $[v^*_{-\mathbf{k}\uparrow}, v^*_{-\mathbf{k}\downarrow}, u^*_{-\mathbf{k}\uparrow}, u^*_{-\mathbf{k}\downarrow}]^T$ with energy $-E_{\mathbf{k}}$. These two states correspond to the same physical solution.

It is easy to show that, in the absence of spin-orbit coupling ($\lambda = 0$), we may explicitly write down the expression for the quasiparticle energy $E_{\mathbf{k}\eta}$. Eq. (15) then recovers the thermodynamic potential of a spin-imbalanced 3D Fermi gas [11].

B. Numerical solutions

For a given set of parameters (i.e., the temperature T, the interaction parameter $1/k_F a_s$ etc.), we solve the order parameter Δ and the FF pairing momentum q by using the self-consistent stationary conditions: $\partial\Omega/\partial\Delta = 0$ and $\partial\Omega/\partial q = 0$, together with the number equation $N = -\partial\Omega/\partial\mu$ for the chemical potential μ. Different saddle-point solutions of these coupled equations give competing ground states. At finite temperatures, the true ground state is the one that has the lowest free energy $F = \Omega + \mu N$.
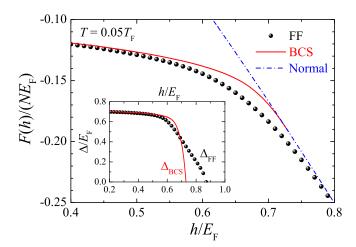
Figure 3: (color online) The free energy of three competing states, including (i) a normal Fermi gas with $\Delta = 0$; (ii) a fully paired BCS superfluid with $\Delta \neq 0$ and $q = 0$; and (iii) a finite-momentum paired FF superfluid with $\Delta \neq 0$ and $q \neq 0$, as a function of the in-plane Zeeman field at resonance and at $T = 0.05T_F$. The Rashba spin-orbit coupling strength is $\lambda k_F / E_F = 1$. The inset shows the Zeeman field dependence of the BCS (red solid line) and FF order parameters (black solid circles).

In numerical calculations, we take the Fermi wave-vector $k_F = (3\pi^2 n_F)^{1/3}$ and the Fermi energy $E_F = \hbar^2 k_F^2/(2m)$ as the units for wave-vector and energy, respectively, in order to make the equations dimensionless. Here, $n_F = N/V$ is the gas density. We focus on the unitary limit with a divergent scattering length $1/(k_F a_s) = 0$. Throughout the paper, we shall use a Rashba spin-orbit coupling strength $\lambda k_F / E_F = 1$. We will consider the superfluid transition temperature as a function of the in-plane Zeeman field, as well as the critical Zeeman field across the Feshbach resonance at a given temperature.

III. RESULTS AND DISCUSSIONS

For any set of parameters, in general there are three competing states: the normal gas ($\Delta = 0$), BCS superfluid ($\Delta \neq 0$ and $q = 0$), and FF superfluid ($\Delta \neq 0$ and $q \neq 0$). These competing states all satisfy the stability condition $\partial^2 \Omega / \partial \Delta^2 \geq 0$ and therefore are stable against phase separation in real space. In Fig. 3, we show the free energy of these states in the unitary limit at $T = 0.05T_F$. It is readily seen that the FF superfluid is always more favorable in energy than the standard BCS superfluid at a finite in-plane Zeeman field, when the Rashba spin-orbit coupling is present. This observation holds for any interaction parameters and temperatures.

At small in-plane Zeeman fields (i.e., $h < 0.5E_F$), the FF superfluid and BCS superfluid are very similar, with essentially the same pairing gap, as shown in the inset of Fig. 3. The difference in the free energy between these

two superfluids is indeed negligible. However, strictly speaking, we always find $\partial \Omega / \partial q < 0$ for the BCS superfluid, indicating that a FF superfluid with a finite center-of-mass momentum q is preferable, although the magnitude of q might be very small. With increasing the Zeeman field, the BCS superfluid ceases to exist. The FF superfluid will also disappear, but at a bit larger critical Zeeman field. This is the so-called Chandrasekhar-Clogston (CC) limit [46, 47], above which a superfluid breaks down. The FF pairing gap vanishes much more smoothly than the BCS pairing gap, as can be seen from the inset of Fig. 3. The phase transition from the FF superfluid to the normal state is continuous.

By collecting the in-plane CC Zeeman field for the FF superfluid state at different finite temperatures, we obtain a finite-temperature phase diagram in the strongly interacting unitary limit, as shown in Fig. 1. For a 2D weakly interacting Fermi gas with Rashba spin-orbit coupling, such a phase diagram has been determined by Barzykin and Gor'kov [18]. At small Zeeman fields $h \sim 0$, we find that

$$[T_c(h = 0) - T_c]/T_c(h = 0) \propto h^2, \qquad (16)$$

in agreement with the analytic expression in Ref. [18]. At the low-temperature regime, the transition temperature $T_c(h)$ is roughly given by

$$T_c(h) \propto [h_c(T = 0) - h]^\alpha, \qquad (17)$$

where $\alpha \simeq 2.5$ and $h_c(T = 0) \simeq 1.05E_F$ is the CC Zeeman field at zero temperature. Our result of $\alpha \simeq 2.5$ seems to be consistent with the analytic prediction of $\alpha = 3$ for a 2D Rashba spin-orbit coupled Fermi gas [18].

In the absence of spin-orbit coupling, the CC Zeeman field at zero temperature is given by $h_c \simeq 1/\sqrt{2}\Delta \simeq 0.707\Delta$ (or $h_c \simeq 0.754\Delta$ with the inclusion of the possibility of a FF superfluid) in the weakly-interacting regime. This is obtain by relating the free energy of a superfluid F_S and of a normal gas F_N through [47],

$$F_N - F_S = \frac{1}{2}\chi h^2, \qquad (18)$$

where χ is the spin susceptibility of a normal gas. In the unitary limit, where the pairing gap Δ is comparable with the Fermi energy E_F, the similar argument within mean-field theory predicts $h_c \simeq 0.693E_F$ [9]. In the presence of spin-orbit coupling, our result of $h_c \simeq 1.05E_F$ seems to be significantly larger. This enhancement of the CC Zeeman field may be understood from the decrease of susceptibility due to Rashba spin-orbit coupling, i.e., it is reduced by a factor of 2 in the weak coupling limit [48]. As shown by Clogston, if the susceptibility is reduced by a fraction α, the CC limit should be divided by $1/\sqrt{\alpha}$ [47]. Thus, by setting $\alpha = 1/2$, the argument by Chandrasekhar and Clogston leads to $h_c \simeq 0.693\sqrt{2}E_F \simeq 0.98E_F$, in a good agreement with our numerical calculation.
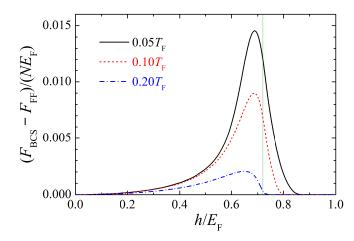
Figure 4: (color online) The free energy difference between the FF superfluid state and the possible BCS superfluid state at resonance and at three different temperatures, $T = 0.05T_F$ (black solid line), $0.10T_F$ (red dashed line), and $0.20T_F$ (blue dot-dashed line). The Rashba spin-orbit coupling strength is $\lambda k_F/E_F = 1$. The BCS state ceases to exist above a Zeeman field $h_{BCS,N} \simeq 0.72E_F$, which depends very weakly on temperature and is indicated by the thin vertical line in the figure. At $h > h_{BCS,N}$, we replace F_{BCS} by F_N in the calculation of the free energy difference.

It is important to note that our phase diagram in Fig. 1 seems to be qualitatively different from the one obtained in the previous study by Zheng and collaborators, which predicts a BCS superfluid at small in-plane Zeeman field [21]. In addition, the CC Zeeman field at zero temperature $h_c(T = 0)$ is shown in their Fig. 1(d) to be about $0.55E_F$ [21], much smaller than what we have obtained numerically, i.e., $h_c(T = 0) \sim 1.05E_F$. The qualitatively different phase diagram is simply due to the different interpretation of the FF state with small pairing momentum. For example, in the calculations by Zheng and collaborators, the FF state with pairing momentum $q < 10^{-3}k_F$ has been regarded as the BCS superfluid [49]. On the other hand, the different CC Zeeman field is probably due to the different accuracy of numerical calculations [49].

A. Temperature dependence of the FF superfluid

We now explore in greater detail the finite-temperature properties of the FF superfluid. Fig. 4 reports the difference in free energy between the FF superfluid state and the BCS superfluid state (the normal state) at three typical temperatures [24]. The energy difference per particle is sizable at low temperatures, suggesting that the FF superfluid is very robust with respect to other competing ground states. The difference becomes considerably smaller with increasing temperature. Nevertheless, it is still visible (i.e., at about $0.002E_F$) at the typical experimental temperature $T = 0.2T_F$. Thus, the thermodynamic stability of the FF superfluid could be guaranteed.
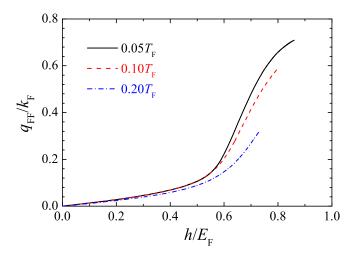

Figure 5: (color online) The pairing momentum of the FF superfluid at resonance and at three different temperatures, $T = 0.05T_F$ (black solid line), $0.10T_F$ (red dashed line), and $0.20T_F$ (blue dot-dashed line). The Rashba spin-orbit coupling strength is $\lambda k_F/E_F = 1$.

More accurately, one may use the so-called Thouless criterion generalized to allow the determination of the FF pairing instability at finite temperatures [50]. Our preliminary result, which partially takes into account the strong pair fluctuations (not shown in the figure), indicates that indeed with decreasing temperature the pairing instability of a normal Fermi gas always occurs at a finite center-of-mass momentum. This is consistent with the mean-field prediction shown in Fig. 4.

Fig. 5 shows the FF pairing momentum as a function of the in-plane Zeeman field at different temperatures. At low Zeeman fields, the pairing momentum is essentially independent on the temperature. At high fields about $0.6E_F$, however, the pairing momentum decreases quickly with increasing temperature. We note that, near zero temperature, the maximum pairing momentum is comparable to the Fermi wave-vector k_F.

Fig. 6 presents the population imbalance between the two spin states, calculated by using $V\delta n = -\partial\Omega/\partial h$ and normalized by the gas density $n_F \equiv k_F^3/(3\pi^2)$. The BCS superfluid state has low capacity to accommodate the population imbalance. Thus, it ceases to exist at a threshold Zeeman field. The deformation of the Fermi surfaces in the FF superfluid state is able to allow more population imbalances. At low temperatures (upper panel, $T = 0.05T_F$), we observe that the population imbalance of the BCS superfluid rises quickly near its threshold Zeeman field, compared with that of the FF superfluid near the CC limit. This distinct behavior might be used to identify the FF superfluid. At a relatively large temperature (low panel, $T = 0.2T_F$), the difference in the population imbalance between the two superfluids is smeared out by temperature.
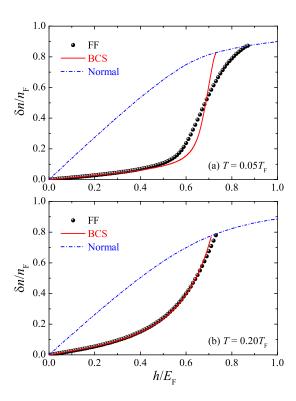
Figure 6: (color online) The number difference between the two spin states at $T = 0.05T_F$ (upper panel) and $T = 0.20T_F$ (lower panel) as a function of the in-plane Zeeman field at resonance and at the spin-orbit coupling strength $\lambda k_F/E_F = 1$. In each panel, the number difference of the three competing states is shown by solid circles (FF), red line (BCS), and blue dot-dashed line (normal Fermi gas).
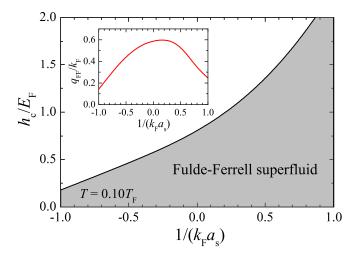

Figure 7: (color online) Phase diagram along the BEC-BCS crossover at $T = 0.10T_F$ and $\lambda k_F/E_F = 1$. The main figure reports the CC Zeeman field at which the FF superfluid phase turns into the normal state. The inset shows the FF pairing momentum at the CC Zeeman field. This figure might be contrasted with the zero temperature result in Ref. [21], see for example, Fig. 1(c) in Ref. [21].

B. FF superfluid across the BEC-BCS crossover

We have so far focused on the resonance limit with $1/(k_F a_s) = 0$. In Fig. 7, we show the CC Zeeman field for the FF superfluid state across the BEC-BCS crossover at the temperature $T = 0.1T_F$. It increases monotonically when the Fermi cloud crosses from the BCS limit to the BEC limit. In the inset, we present the FF pairing momentum at the CC Zeeman field. There is a maximum in the pairing momentum at about the Feshbach resonance, due to the competition between the many-body and two-body effects. The initial increase of the FF pairing momentum on the BCS side arises from the many-body effect. Towards the BEC limit, however, the two-body effect becomes dominant and the FF pairing momentum decreases gradually to the center-of-mass momentum of the two-particle bound state. In the previous study by Dong and collaborators, the many-body and two-body predictions for the FF pairing momentum have been compared with each other for a 3D Fermi gas with 3D isotropic spin-orbit coupling [34]. Our result in the inset is consistent with their predictions.

IV. CONCLUSIONS

In summary, we have investigated the finite-temperature phase diagram of a three dimensional atomic Fermi gas with Rashba spin-orbit coupling and in-plane Zeeman field near a broad Feshbach resonance. We have shown that its superfluid state is always an inhomogeneous Fulde-Ferrell superfluid, if the spin-orbit coupling is sufficiently large.

Our work complements the previous studies with spin-orbit coupled Fermi systems in the solid-state, which are described by essentially the same model Hamiltonian in the weakly interacting regime [18–20]. Our mean-field treatment gives a qualitative picture of the Fulde-Ferrell superfluidity in the strongly interacting resonance limit, which is of great interest and of experimental relevance.

Our result extends the previous zero-temperature investigation by Zheng and collaborators [21] to finite temperatures. In particular, we have clarified that the BCS superfluid found by these authors at small in-plane Zeeman fields is better understood as the Fulde-Ferrell superfluid with small pairing momentum. Our finite-temperature calculations indicate that the Fulde-Ferrell superfluidity could be observable at about $T \sim 0.2T_F$, a temperature that is already reached in current cold-atom experiments when the spin-orbit coupling is absent [24].

Our investigation is based on the mean-field theory, which is known to provide qualitative picture of the BEC-BCS crossover. The strong pair fluctuations in a strongly interacting Fulde-Ferrell superfluid might be taken into account by using many-body T-matrix theories [50–52]. This is to be addressed in the future work. Our preliminary analysis indicates that the superfluid transition temperature predicted in Fig. 1 will decrease by a factor of

about 2 at the typical in-plane Zeeman field $h = 0.6E_F$.

Appendix A: Rashba spin-orbit Hamiltonian

In the literature, the Rashba spin-orbit coupling and in-plane Zeeman field is commonly written as $\lambda(\sigma_y \hat{k}_x - \sigma_x \hat{k}_y) - h\sigma_x$ [21]. Here we show that our single-particle Hamiltonian Eq. (5) uses exactly the same Rashba-type spin-orbit coupling and in-plane Zeeman field, after some rotations in real space or spin space.

For this purpose, we first perform the rotation of real space along the x-axis: $x \to x$, $y \to -z$, and $z \to y$. As the result, the single-particle Hamiltonian Eq. (5) becomes,

$$\begin{bmatrix} \psi_\uparrow^\dagger, \psi_\downarrow^\dagger \end{bmatrix} \begin{bmatrix} \hat{\xi}_{\mathbf{k}} + \lambda \hat{k}_y + h & \lambda \hat{k}_x \\ \lambda \hat{k}_x & \hat{\xi}_{\mathbf{k}} - \lambda \hat{k}_y - h \end{bmatrix} \begin{bmatrix} \psi_\uparrow \\ \psi_\downarrow \end{bmatrix}. \quad \text{(A1)}$$

In the second step, let us take a unitary transformation,

$$\psi_\uparrow(\mathbf{x}) = \frac{1}{\sqrt{2}} \left[\phi_\uparrow(\mathbf{x}) - \phi_\downarrow(\mathbf{x}) \right], \quad \text{(A2)}$$

$$\psi_\downarrow(\mathbf{x}) = \frac{1}{\sqrt{2}} (-i) \left[\phi_\uparrow(\mathbf{x}) + \phi_\downarrow(\mathbf{x}) \right]. \quad \text{(A3)}$$

It is straightforward to check that under such a transformation, the single-particle Hamiltonian changes to,

$$\begin{bmatrix} \phi_\uparrow^\dagger, \phi_\downarrow^\dagger \end{bmatrix} \begin{bmatrix} \hat{\xi}_{\mathbf{k}} & -i\lambda\hat{k}_x - \lambda\hat{k}_y - h \\ i\lambda\hat{k}_x - \lambda\hat{k}_y - h & \hat{\xi}_{\mathbf{k}} \end{bmatrix} \begin{bmatrix} \phi_\uparrow \\ \phi_\downarrow \end{bmatrix}, \quad \text{(A4)}$$

which precisely has the form of $\lambda(\sigma_y \hat{k}_x - \sigma_x \hat{k}_y) - h\sigma_x$.

The interaction Hamiltonian Eq. (6) is not apparently affected by the spatial rotation. Furthermore, as $\psi_\downarrow(\mathbf{x}) \psi_\uparrow(\mathbf{x}) = -i\phi_\downarrow(\mathbf{x}) \phi_\uparrow(\mathbf{x})$, it is also not affected by the unitary transformation. For the FF pairing momentum, we can see that the direction along the z-axis is fully equivalent to the direction of y-axis after the two rotations. Thus, our assumed z-axis for the FF pairing momentum is consistent with the observation by Zheng and collaborators [21] and by Barzykin and Gor'kov [18], that the FF pairing momentum with $\lambda(\sigma_y \hat{k}_x - \sigma_x \hat{k}_y) - h\sigma_x$ is along the y-axis.

[1] P. Fulde and R. A. Ferrell, Phys. Rev. **135**, A550 (1964).
[2] A. I. Larkin and Y. N. Ovchinnikov, Zh. Eksp. Teor. Fiz. **47**, 1136 (1964) [Sov. Phys. JETP **20**, 762 (1965)].
[3] R. Casalbuoni and G. Nardulli, Rev. Mod. Phys. **76**, 263 (2004).
[4] L. Radzihovsky and D. E. Sheehy, Rep. Prog. Phys. **73**, 076501 (2010).
[5] K. B. Gubbels and H. T. C. Stoof, Phys. Rep. **525**, 4, 255 (2013).
[6] H. A. Radovan, N. A. Fortune, T. P. Murphy, S. T. Hannahs, E. C. Palm, S. W. Tozer, and D. Hall, Nature (London) **425**, 51 (2003).
[7] S. Uji, T. Terashima, M. Nishimura, Y. Takahide, T. Konoike, K. Enomoto, H. Cui, H. Kobayashi, A. Kobayashi, H. Tanaka, M. Tokumoto, E. S. Choi, T. Tokumoto, D. Graf, and J. S. Brooks, Phys. Rev. Lett. **97**, 157001 (2006).
[8] M. Kenzelmann, Th. Strï¿œssle, C. Niedermayer, M. Sigrist, B. Padmanabhan, M. Zolliker, A. D. Bianchi, R. Movshovich, E. D. Bauer, J. L. Sarrao, and J. D. Thompson, Science **321**, 1652 (2008).
[9] D. E. Sheehy and L. Radzihovsky, Phys. Rev. Lett. **96**, 060401 (2006).
[10] L. He, M. Jin, and P. Zhuang, Phys. Rev. B **73**, 214527 (2006).
[11] H. Hu and X.-J. Liu, Phys. Rev. A **73**, 051603(R) (2006).
[12] G. Orso, Phys. Rev. Lett. **98**, 070402 (2007).
[13] H. Hu, X.-J. Liu, and P. D. Drummond, Phys. Rev. Lett. **98**, 070403 (2007).
[14] X. W. Guan, M. T. Batchelor, C. Lee, and M. Bortz, Phys. Rev. B **76**, 085120 (2007).
[15] X.-J. Liu, H. Hu, and P. D. Drummond, Phys. Rev. A **76**, 043605 (2007).
[16] X.-J. Liu, H. Hu, and P. D. Drummond, Phys. Rev. A **78**, 023601 (2008).
[17] Y.-A. Liao, A. S. C. Rittner, T. Paprotta, W. Li, G. B. Partridge, R. G. Hulet, S. K. Baur, and E. J. Mueller, Nature **467**, 567 (2010).
[18] V. Barzykin and L. P. Gor'kov, Phys. Rev. Lett. **89**, 227002 (2002).
[19] Ol'ga Dimitrova and M. V. Feigel'man, Phys. Rev. B **76**, 014522 (2007).
[20] D. F. Agterberg and R. P. Kaur, Phys. Rev. B **75**, 064511 (2007).
[21] Z. Zheng, M. Gong, X. Zou, C. Zhang, and G.-C. Guo, Phys. Rev. A **87**, 031602(R) (2013).
[22] Z. Zheng, M. Gong, Y. Zhang, X. Zou, C. Zhang, and G.-C. Guo, arXiv:1212.6826 (2012).
[23] I. Bloch, J. Dalibard, and W. Zwerger, Rev. Mod. Phys. **80**, 885 (2008).
[24] M. J. H. Ku, A. T. Sommer, L. W. Cheuk, and M. W. Zwierlein, Science **335**, 563 (2012).
[25] H. Burkhardt and D. Rainer, Ann. Phys. (Berlin) **3**, 181 (1994).
[26] N. Yoshida and S.-K. Yip, Phys. Rev. A **75**, 063601 (2007).

[27] A. Bulgac and M. M. Forbes, Phys. Rev. Lett. **101**, 215301 (2008).

[28] P. Wang, Z.-Q. Yu, Z. Fu, J. Miao, L. Huang, S. Chai, H. Zhai, and J. Zhang, Phys. Rev. Lett. **109**, 095301 (2012).

[29] L. W. Cheuk, A. T. Sommer, Z. Hadzibabic, T. Yefsah, W. S. Bakr, and M. W. Zwierlein, Phys. Rev. Lett. **109**, 095302 (2012).

[30] H. Hu, H. Pu, J. Zhang, S.-G. Peng, and X.-J. Liu, Phys. Rev. A **86**, 053627 (2012).

[31] V. B. Shenoy, arXiv:1211.1831 (2012).

[32] X.-J. Liu and H. Hu, Phys. Rev. A **87**, 051608(R) (2013).

[33] F. Wu, G.-C. Guo, W. Zhang, and W. Yi, Phys. Rev. Lett. **110**, 110401 (2013).

[34] L. Dong, L. Jiang, and H. Pu, New J. Phys. **15**, 075014 (2013).

[35] X.-F. Zhou, G.-C. Guo, W. Zhang, and W. Yi, Phys. Rev. A **87**, 063606 (2013).

[36] J. D. Sau, R. Sensarma, S. Powell, I. B. Spielman, and S. Das Sarma, Phys. Rev. B **83**, 140510(R) (2011).

[37] B. M. Anderson, I. B. Spielman, and G. Juzeliūnas, arXiv:1306.2606 (2013).

[38] B. M. Anderson, G. Juzeliūnas, I. B. Spielman, and V. M. Galitski, Phys. Rev. Lett. **108**, 235301 (2012).

[39] A. Kubasiak, P. Massignan, and M. Lewenstein, Euro-phys. Lett. **92**, 46004 (2010).

[40] J. P. Vyasanakere, S. Zhang, and V. B. Shenoy, Phys. Rev. B **84**, 014512 (2011).

[41] H. Hu, L. Jiang, X. -J. Liu and H. Pu, Phys. Rev. Lett. **107**, 195304 (2011).

[42] Z.-Q. Yu, and H. Zhai, Phys. Rev. Lett. **107**, 195305 (2011).

[43] L. Jiang, X.-J. Liu, H. Hu, and H. Pu, Phys. Rev. A **84**, 063618 (2011).

[44] J. P. Vyasanakere, and V. B. Shenoy, New J. Phys. **14**, 043041 (2012).

[45] L. Dong, L. Jiang, H. Hu, and H. Pu, Phys. Rev. A **87**, 043616 (2013).

[46] B. S. Chandrasekhar, Appl. Phys. Lett. **1**, 7 (1962).

[47] A. M. Clogston, Phys. Rev. Lett. **9**, 226 (1962).

[48] L. P. Gor'kov and E. I. Rashba, Phys. Rev. Lett. **87**, 037004 (2001).

[49] Z. Zheng and X. Zou, private communication.

[50] X.-J. Liu and H. Hu, Europhys. Lett. **75**, 364 (2006).

[51] H. Hu, X.-J. Liu, and P. D. Drummond, Europhys. Lett. **74**, 574 (2006).

[52] H. Hu, X.-J. Liu, and P. D. Drummond, Phys. Rev. A **77**, 061605(R) (2008).